

# Simulation and Design of Step-Etched Junction Termination Extensions for GaN Power Diodes

SAND2020-0661C

Jeramy R. Dickerson, Andrew T. Binder, Greg Pickrell, Brendan P. Gunning, and Robert J. Kaplar  
Sandia National Laboratories, Albuquerque, NM 87185 USA  
e-mail: jrdicke@sandia.gov; phone: +1-505-845-8619

**Abstract**—Proper edge termination is required to reach large blocking voltages in vertical power devices. Limitations in selective area p-type doping in GaN restrict the types of structures that can be used for this purpose. A junction termination extension (JTE) can be employed to reduce field crowding at the junction periphery where the charge in the JTE is designed to sink the critical electric field lines at breakdown. One practical way to fabricate this structure in GaN is by a step-etched single-zone or multi-zone JTE where the etch depths and doping levels are used to control the charge in the JTE. The multi-zone JTE is beneficial for increasing the process window and allowing for more variability in parameter changes while still maintaining a designed percentage of the ideal breakdown voltage. Impact ionization parameters reported in literature for GaN are compared in a simulation study to ascertain the dependence on breakdown performance. Two 3-zone JTE designs utilizing different impact ionization coefficients are compared. Simulations confirm that the choice of impact ionization parameters affects both the predicted breakdown of the device as well as the fabrication process variation tolerance for a multi-zone JTE. Regardless of the impact ionization coefficients utilized, a step-etched JTE has the potential to provide an efficient, controllable edge termination design.

**Keywords**—GaN, edge termination, vertical power diode, multi-zone JTE, JTE

## I. INTRODUCTION

Recent commercial availability of native gallium nitride (GaN) substrates is enabling research on vertical GaN-based power devices [1]. Gallium nitride power semiconductor devices are commercially available from several vendors [2]–[6] but are so far constrained to a lateral device architecture which limits the maximum blocking voltage to less than 1 kV and restricts the achievable maximum current due to the large physical die size required for high current lateral devices [1]. In contrast, a vertical device architecture enables blocking voltages of nearly 5 kV [7–8] and greater current output for the same die size, making the vertical device architecture more desirable for power semiconductor devices.

One of the principal design challenges for vertical power devices is the management of electric fields at the periphery. Breakdown voltage values can be severely reduced by electric field crowding. A proper edge termination design can increase the breakdown voltage by spreading the electric field and avoiding field enhancement effects.

Several techniques exist to protect the junction including floating guard rings, junction termination extension (JTE), and beveled edge termination [9]–[10]. Junction termination for GaN-based vertical power devices is complicated by

---

Sandia National Laboratories is a multi-mission laboratory managed and operated by National Technology & Engineering Solutions of Sandia, LLC, a wholly owned subsidiary of Honeywell International Inc., for the U.S. Department of Energy's National Nuclear Security Administration under contract DE-NA0003525. This paper describes objective technical results and analysis. Any subjective views or opinions that might be expressed in the paper do not necessarily represent the views of the U.S. Department of Energy or the United States Government.

limitations in selective-area p-type doping [11]. This limitation necessitates further innovation to create structures such as floating guard rings or junction termination extensions in which the total charge of the p-type edge termination is critically important.

Section II will introduce the theory of the JTE in the context of GaN devices. Additionally, the difference in several state-of-the-art impact ionization (II) coefficients will be discussed. Section III will describe the design space of a multi-zone JTE. Section IV will provide a summary of the results.

## II. SINGLE-ZONE JTE

Edge terminations are required to control the electric fields near the pn junction and to prevent premature breakdown of devices. One possible method to control edge termination charge is by means of counter-doping the p-GaN with Si to compensate the region [12]. Another possibility is to use nitrogen ion implantation which makes the region semi-insulating [13], thereby controlling the total dose in the edge termination. The focus of this paper is on the use of a junction termination extension (JTE) [14–16]. Typically, JTE structures are fabricated by dopant implantation at the surface of the device. However, due to the present difficulty of implanting Mg in GaN, an alternative method would be to selectively etch back the p-GaN region to a target thickness. The JTE total dose is then the doping concentration and thickness product of the remaining p-type material.

If designed correctly, the JTE can terminate the field lines and allow the breakdown to approach the planar-junction theoretical limit [17]. According to Gauss's law, the electric flux through any closed surface is equal to the total charge inside the volume bounded by the surface divided by the permittivity (Eq. 1).

$$\phi = E \cdot A = \frac{\sigma \cdot A}{\epsilon_r \cdot \epsilon_0} \quad (1)$$

In this equation,  $\phi$  is the electric flux,  $\epsilon$  is the permittivity,  $A$  is the area of the Gaussian surface,  $E$  is the electric field, and  $\sigma$  is the charge per unit area which is also equal to the JTE charge,  $n_{JTE}$ , times the elementary charge  $q$  (Eq. 2).

$$\sigma = n_{JTE} \cdot q \quad (2)$$

This equation can be rearranged to show the JTE charge required to terminate the critical electric field at breakdown (Eq. 3).

$$n_{JTE} = \frac{E_{crit} \cdot \epsilon_r \cdot \epsilon_0}{q} \quad (3)$$

By allowing the remaining etched p-region and total Mg concentration product to equal the JTE charge, the field termination will be optimized. Equation 3 shows that the dose needed to optimize the JTE design is a function of the critical field, which in turn depends on the impact ionization (II) parameters of the material. The impact ionization parameters for GaN are still under investigation, and several recent papers have attempted to experimentally determine these as a fit to an impact ionization model (Eq. 4).

TABLE I. IMPACT IONIZATION PARAMETERS FOR GAN

Reference	Electrons		Holes	
	$\alpha_0$ (cm <sup>-1</sup> )	$\varepsilon_0$ (V/cm)	$\alpha_0$ (cm <sup>-1</sup> )	$\varepsilon_0$ (V/cm)
Cao et al. [18]	$4.48 \times 10^8$	$3.39 \times 10^7$	$7.13 \times 10^6$	$1.46 \times 10^7$
Ji et al. [19]	$2.11 \times 10^9$	$3.69 \times 10^7$	$4.39 \times 10^6$	$1.80 \times 10^7$
Maeda et al. [14] <sup>a</sup>	$1.30 \times 10^6$	$1.18 \times 10^7$	$1.30 \times 10^6$	$1.18 \times 10^7$

<sup>a</sup> Evaluated at room temperature

$$\alpha = \alpha_0 \cdot e^{-\left(\frac{\varepsilon_0}{\varepsilon}\right)} \quad (4)$$

Table I shows some of the more recent impact ionization coefficient parameter values found in the literature. At a drift region net carrier concentration of  $2 \times 10^{16}$  cm<sup>-3</sup> and a relative permittivity value of 9.0, these parameters correspond to critical fields values of 2.84, 3.14, and 2.46 MV/cm for Cao, Ji, and Maeda respectively [18-20].

Fig. 1 shows the device layout for simulations of a single-zone etched JTE. The diode drift region thickness was set to 10  $\mu$ m with a  $2 \times 10^{16}$  n-type net carrier concentration. This is expected to be a non-punch-through design for all parameter sets in Table I. The p-region consists of a 400 nm thick epitaxial layer uniformly doped at  $10^{18}$  cm<sup>-3</sup> [Mg], capped with a 100 nm thick layer uniformly doped at  $3 \times 10^{19}$  cm<sup>-3</sup> [Mg] to assist in forming a good p-type contact. The JTE thickness,  $t_1$ , was set to 260 nm. A final etch down to the pn junction, next to the JTE region, is designed to represent isolation between devices. Simulations were performed using SILVACO TCAD software [21].

The value of the JTE dose,  $n_{JTE}$ , can be changed by either altering the doping or the thickness of the JTE region. Fig. 2 indicates the change in device breakdown voltage as a function of p-layer doping for fixed thickness. A similar plot can be obtained by holding the p-doping constant and varying the thickness of the p-region layer. In either case the result is a sharply peaked profile, indicating a narrow window for process variations. Additionally, two important concepts can be taken from the results shown in Fig. 2. First, the critical fields vary dramatically between the different II parameter sets leading to a 480 V difference in possible breakdown voltage values. A second and more subtle point is the

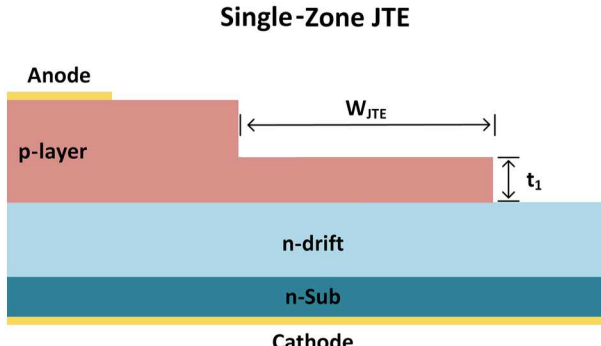


Fig. 1 A single-etch JTE design (not to scale).  $W_{JTE}$  is set to 20  $\mu$ m and  $t_1$  is 260 nm. The dose,  $n_{JTE}$ , of the JTE layer can be altered by varying the p-layer doping. Alternatively, the thickness,  $t_1$ , can be altered to obtain similar results. For example, doubling the thickness of  $t_1$  is equivalent to doubling the Mg concentration in the p-layer.

difference in the tolerance of breakdown voltage as a function of total dose for each parameter set. This will be explored in more detail in the following section.

### III. MULTI-ZONE JTE

As can be seen in Fig. 1, a single JTE presents a rather challenging fabrication tolerance, in that variations in JTE dose can dramatically lower the breakdown voltage. For instance, on the blue curve, a [Mg] concentration increase from  $6.4 \times 10^{17}$  to  $1.0 \times 10^{18}$  cm<sup>-3</sup> drops the breakdown voltage in half from 1261 to 630 V. Additionally, surface etch damage and surface charge effects add another level of complexity and will be the subject of future work. To accommodate for

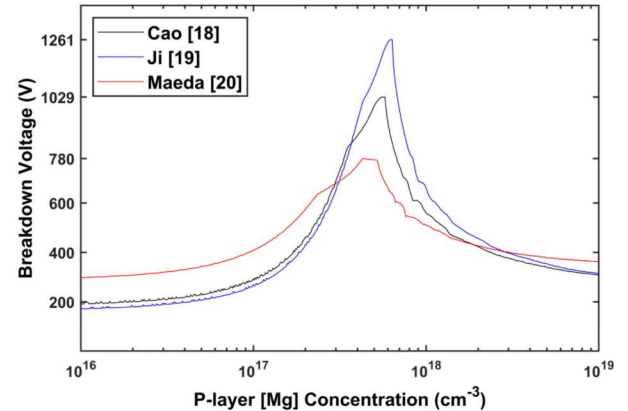


Fig. 2. Device breakdown as a function of p-layer [Mg] doping for a single-zone JTE. A peak breakdown voltage is achieved when the value of  $n_{JTE}$  follows equation (3). The value of  $E_{crit}$  in each case is determined by the impact ionization parameters from Table I.

variation in these factors, it is common to implement a multi-zone step-etched JTE (MZ-JTE) as shown in Fig. 3. The MZ-JTE aims to reduce sensitivity to process variation by employing several JTEs, each with a discrete total charge.

Two 3-zone designs are demonstrated in Fig. 4. The first design utilizes the II coefficients of Ji [19], with  $t_1$ ,  $t_2$ , and  $t_3$  equal to 260, 151, and 93 nm respectively. The second design utilizes the II coefficients of Maeda [20], with  $t_1$ ,  $t_2$ , and  $t_3$  equal to 260, 91, and 32 nm respectively. These designs were chosen to ensure a minimum breakdown voltage threshold of at least 80% between the peak breakdown voltage values as seen in Fig. 4. It should be noted that the [Mg] profile is the

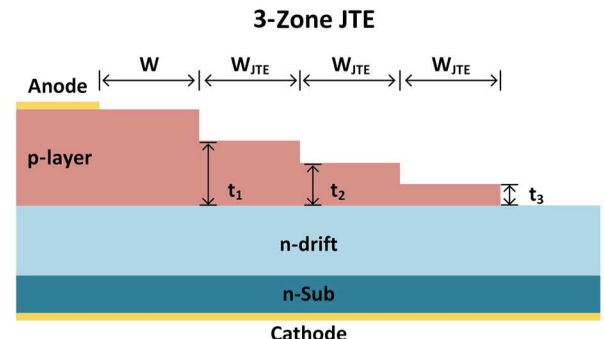


Fig. 3 A 3-etch JTE design (not to scale).  $W_{JTE}$  is set to 20  $\mu$ m and the values of  $t_1$ ,  $t_2$ , and  $t_3$  in conjunction with the p-layer Mg concentration determine the total dose,  $n_{JTE}$ , for each zone, with the intent of increasing the fabrication tolerance of the design. The different etch depths can be designed to provide a minimum allowable threshold for the breakdown voltage.

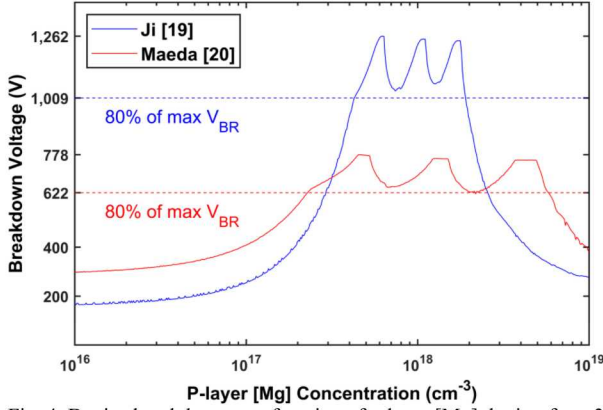


Fig. 4. Device breakdown as a function of p-layer [Mg] doping for a 3-zone JTE. The value of  $n_{JTE}$  is optimal at three doping concentrations. The distance between peaks as a function of doping can be modified by altering the values of  $t_1$ ,  $t_2$ , and  $t_3$  from Fig. 3.

same for each JTE region. It is the difference in etch depths that achieve the desired dose for each region. This is in contrast to MZ-JTEs fabricated in SiC, for instance, where the dose is controlled by implant and no etch is required.

The subtlety mentioned in Section II concerning the tolerance of the different II coefficients is more obvious here. While the II coefficients of Ji indicate a tolerance range in doping of  $4.4 \times 10^{17}$  to  $1.8 \times 10^{18} \text{ cm}^{-3}$ , the parameters of Maeda indicate a tolerance range of  $2.4 \times 10^{17}$  to  $6.0 \times 10^{18} \text{ cm}^{-3}$ , nearly twice the range. A third design using the II coefficients of Cao [18] is not shown here as the results simply lie between the other two sets of II coefficients in terms of both the tolerance with doping range and breakdown voltage. Despite the differences seen in the II parameters, it should be noted that altering the minimum breakdown voltage threshold inversely affects the tolerance range.

The electric field profiles at breakdown are displayed in Fig. 5 for the II parameters of Ji [19]. Figs. 5 (a) and (e) are for p-region [Mg] doping concentrations of  $10^{17} \text{ cm}^{-3}$  and  $10^{19} \text{ cm}^{-3}$  respectively. In the former case, the  $3 \times 10^{19} \text{ cm}^{-3}$  layer leads to field crowding effects and breakdown prior to the electric field penetration into the JTE regions. For the latter case, the [Mg] concentration is too high and the JTE regions remain largely un-depleted resulting in field crowding and premature breakdown.

Figs. 5 (b), (c), and (d) indicate the field profiles for the three peak breakdown values and corresponding doping levels indicated by the blue curve in Fig. 4. For instance, the thickest JTE region corresponds to the lightest dose or the leftmost peak in Fig. 4. During fabrication the Mg concentration will remain uniform laterally across the device. Therefore, the target Mg concentration should correspond to the middle JTE design, in this case 151 nm at  $1.1 \times 10^{19} \text{ cm}^{-3}$ . The purpose of the other two JTE regions is to allow for a wider range in growth and fabrication variations, not to increase the breakdown voltage.

While not shown here, alterations in the individual values  $t_1$ ,  $t_2$ , and  $t_3$  will affect the optimal value of  $n_{JTE}$  for each JTE zone. Increasing the value of  $t$  for any zone will shift the peak to the left and decreasing it will shift the peak to the right.

The widths of the JTE regions,  $W_{JTE}$ , should be sufficiently large to ensure spreading of the electric field lines. Fig. 6 shows the breakdown vs.  $W_{JTE}$  width for the Ji II

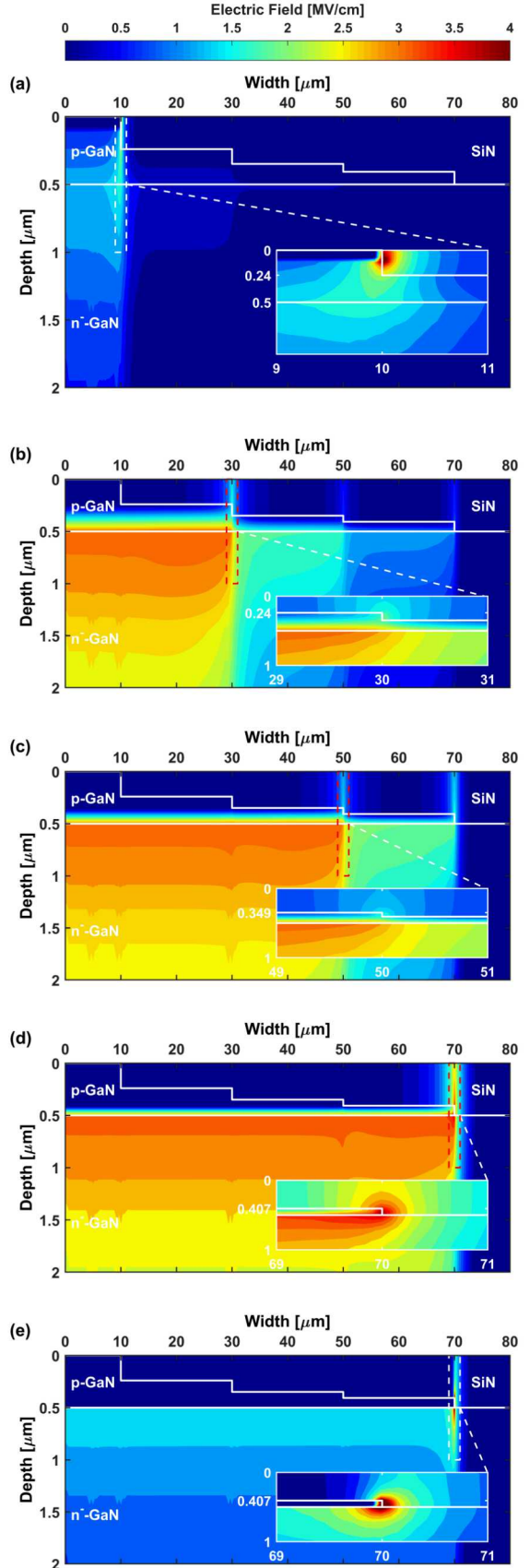


Fig. 5. Electric field profile for p-GaN [Mg] =  $10^{17} \text{ cm}^{-3}$  (a),  $6.3 \times 10^{17} \text{ cm}^{-3}$  (b),  $1.1 \times 10^{18} \text{ cm}^{-3}$  (c),  $1.7 \times 10^{18} \text{ cm}^{-3}$  (d), and  $10^{19} \text{ cm}^{-3}$  (e). Sub plots (b), (c), and (d) correspond to blue curve peaks, from left to right, in Fig. 4 respectively. As can be seen in these three sub-plots, the electric field is nearly planar at breakdown, indicating an optimal JTE design.

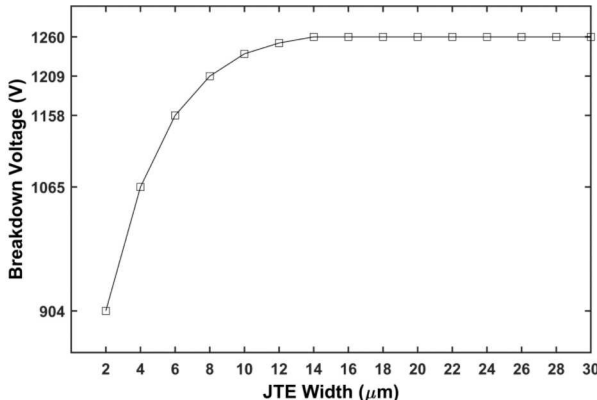


Fig. 6. Device breakdown as a function of  $W_{JTE}$  for an optimal  $n_{JTE}$  using the II parameters of Ji [19]. At 14  $\mu\text{m}$  width, the maximum breakdown voltage is achieved.

coefficients. At 14  $\mu\text{m}$  width the breakdown voltage achieves its maximum value, and increasing the width maintains this value. A value of 20  $\mu\text{m}$  was used in this paper to follow the approximate rule that the  $W_{JTE}$  width should be double the depletion region thickness at breakdown [18].

#### IV. CONCLUSION

Etching a MZ-JTE has potential to increase the effectiveness of the edge termination by allowing a more precise control of the JTE dose. The values of II parameters used can alter the fabrication tolerance of a MZ-JTE design. Future work will investigate the impact of surface charges from oxide traps and etch damage. Additionally, MZ-JTE devices are currently being fabricated at Sandia National Laboratories and will be studied to determine the effect of etched JTE designs on device breakdown.

#### REFERENCES

- [1] J. Hu, Y. Zhang, M. Sun, D. Piedra, N. Chowdhury, and T. Palacios, "Materials and processing issues in vertical GaN power electronics," *Mater. Sci. Semicond. Process.*, vol. 78, pp. 75–84, May 2018.
- [2] "GaN Power Transistor Products | GaN Systems." [Online]. Available: <https://gansystems.com/gan-transistors/>. [Accessed: 04-Dec-2019].
- [3] "Gallium Nitride (GaN) ICs and Semiconductors – EPC." [Online]. Available: <https://epc-co.com/epc>. [Accessed: 04-Dec-2019].
- [4] "GaN Power Devices - Industrial Devices & Solutions - Panasonic." [Online]. Available: <https://industrial.panasonic.com/ww/products/semiconductors/powerics/ganpower>. [Accessed: 04-Dec-2019].
- [5] "Navitas | Creator of GaNFast." [Online]. Available: <https://www.navitassemi.com/>. [Accessed: 04-Dec-2019].
- [6] "Gallium Nitride (GaN) Power Devices - Transphorm." [Online]. Available: <https://www.transphormusa.com/en/>. [Accessed: 04-Dec-2019].
- [7] H. Ohta, K. Hayashi, F. Horikiri, M. Yoshino, T. Nakamura, and T. Mishima, "5.0kV breakdown-voltage vertical GaN p-n junction diodes," *Jpn. J. Appl. Phys.*, vol. 57, no. 4, pp. 4–09, 2018.
- [8] H. Ohta, N. Asai, F. Horikiri, Y. Narita, T. Yoshida, and T. Mishima, "Two-Step Mesa Structure GaN p-n Diodes with Low On-resistance, High Breakdown Voltage and Excellent Avalanche Capabilities," *In Press*.
- [9] B. J. Baliga, *Fundamentals of power semiconductor devices*. Boston, MA: Springer US, 2008.
- [10] A. T. Binder *et al.*, "Bevel Edge Termination for Vertical GaN Power Diodes," in *The 7th Workshop on Wide Bandgap Power Devices and Applications (WiPDA 2019)*, 2019, pp. 281–285.
- [11] M. J. Tadjer *et al.*, "Selective p-type Doping of GaN:Si by Mg Ion Implantation and Multicycle Rapid Thermal Annealing," *ECS J. Solid State Sci. Technol.*, vol. 5, no. 2, pp. P124–P127, Dec. 2016.
- [12] M. Shurraab, A. Siddiqui, and S. Singh, "Counter-Doped Multizone Junction Termination Extension Structures in Vertical GaN Diodes," *IEEE J. Electron Devices Soc.*, vol. 7, pp. 261–267, 2019.
- [13] J. R. Dickerson *et al.*, "Vertical GaN Power Diodes With a Bilayer Edge Termination," *IEEE Trans. Electron Devices*, vol. 63, no. 1, p. 419, 2016.
- [14] V. A. K. Temple and M. S. Adler, "The theory and application of a simple etch contour for near ideal breakdown voltage in plane and planar pn junctions," *IEEE Trans. Electron Devices*, vol. 23, no. 8, pp. 950–955, 1976.
- [15] V. A. K. Temple, "Junction termination extension (JTE), A new technique for increasing avalanche breakdown voltage and controlling surface electric fields in P-N junctions," 1977, pp. 423–426.
- [16] V. A. K. Temple and W. Tantraporn, "Junction Termination Extension for Near-Ideal Breakdown Voltage in p-n Junctions," *IEEE Trans. Electron Devices*, vol. 33, no. 10, pp. 1601–1608, 1986.
- [17] B. J. Baliga, "High-voltage device termination techniques a comparative review." IEE Proceedings I (Solid-State and Electron Devices) 129, no. 5 (1982): 173–179.
- [18] L. Cao *et al.*, "Experimental characterization of impact ionization coefficients for electrons and holes in GaN grown on bulk GaN substrates," *Appl. Phys. Lett.*, vol. 112, no. 26, 2018.
- [19] D. Ji, B. Ercan, and S. Chowdhury, "Experimental determination of impact ionization coefficients of electrons and holes in gallium nitride using homojunction structures," *Appl. Phys. Lett.*, vol. 115, no. 7, 2019.
- [20] T. Maeda *et al.*, "Measurement of avalanche multiplication utilizing Franz-Keldysh effect in GaN p-n junction diodes with double-side-depleted shallow bevel termination," *Appl. Phys. Lett.*, vol. 115, no. 14, 2019.
- [21] Silvaco, Inc. (2019). Atlas User Manual Device Simulation Software. [Online]. Available: <http://www.silvaco.com>
- [22] T. Kimoto and J. A. Cooper, *Fundamentals of Silicon Carbide Technology*. Wiley, 2014.